

Observation of coherence revival and fidelity saturation in a δ -kicked rotor potential

Saijun Wu,* Alexey Tonyushkin, and Mara G. Prentiss

Department of Physics, Harvard University, Cambridge, MA, 02138

(Dated: November 21, 2018)

Abstract

We experimentally investigate the effect of atomic δ -kicked rotor potentials on the mutual coherence between wavepackets in an atom interferometer. The differential action of the kicked rotor degrades the mutual coherence, leading to a reduction of the interferometry fringe visibility; however, when the repetition rate of the kicked rotor is at or near the quantum resonance, we observe revival of matter-wave coherence as the number of kicks increases, resulting in non-vanishing coherence in the large kick number limit. This coherence saturation effect reflects a saturation of fidelity decay due to momentum displacements in deep quantum regime. The saturation effect is accompanied with an invariant distribution of matter-wave coherence under the kicked rotor perturbations.

PACS numbers: 05.45.Mt, 32.80.Lg, 39.20.+q, 03.75.dg

Information about the stability of quantum evolution in response to small perturbations is of both fundamental and practical importance. At a fundamental level, the study of quantum stability elucidates how quantum irreversibility emerges from the unitary wave evolution governed by the Schrödinger equation [1]. At a technological level, quantum control is implementable only if the quantum trajectories are stable against small parameter errors. Quantum stability is best characterized by a decay of fidelity which gives the squared overlap between a perturbed quantum trajectory with its unperturbed copy [1]. In contrast with the generic Lyapunov decay of fidelity characteristic of classically chaotic systems [2, 3], corresponding quantum systems can survive certain types of perturbations over long time, leading to quantum freeze or saturation of fidelity decay [4, 5, 6]. Quantum fidelity decay is practically related to interferometry experiments [7, 8, 9, 10], where the perturbation under investigation differentially perturbs two quantum trajectories in the interferometer and reduces the overlap at the interferometry output. We shall generally consider a beamsplitter operation $\hat{S} \sim 1 + \hat{D}$ applied at $t = 0$ that puts an atom into a superposition of two quantum trajectories at $0 < t < T$: the “original” trajectory $e^{-i\hat{H}_0 t}|\psi\rangle$ and the “shifted” trajectory $e^{-i\hat{H}_0 t}\hat{D}|\psi\rangle$ where \hat{H}_0 is a perturbation-free Hamiltonian. With additional interferometry operations (mirrors and beamsplitters) to create an effective time-reversal, the two trajectories can be optimally overlapped at the interferometry output. The perturbation \hat{V} applied at $0 < t < T$ can be written in the frame of the “original” and “shifted” states as $\hat{V}_1 = \hat{V}$ and $\hat{V}_2 = \hat{D}^{-1}\hat{V}\hat{D}$ respectively. The trajectory overlap A at the interferometry output is expected to reduce to \tilde{A} due to the differential perturbation. The ratio \tilde{A}/A gives the fidelity amplitude $f = \langle\psi|\hat{U}_2^{-1}(T)\hat{U}_1(T)|\psi\rangle$ with $\hat{U}_{1,2}(T) = \hat{T}e^{-i\int_0^T \hat{V}_{1,2} dt}$ in the interaction picture (\hat{T} the time-ordering operator) [4].

Much of the earlier experimental work studied the fidelity decay with internal-state echoes [7, 8, 9, 10] where \hat{D} is associated with an internal-state operation and $\hat{V}_{1,2}$ correspond to perturbations in different internal states. In particular, a Ramsey interferometer was suggested in ref. [11] to study the stability of an atomic δ -kicked rotor (ADKR), which is an atom-optics realization of a δ -kicked rotor by subjecting cold atoms to periodic “kicks” from an optical standing wave (SW) pulse train [12]. Classical dynamics of a δ -kicked rotor is described by the standard map, which displays generic features of classical instabilities [2].

Quantum dynamics of ADKR is strongly affected by two relevant frequencies, the repetition rate of the pulses and the atomic recoil frequency. A quantum resonance happens when the two frequencies coincide, where dynamics of atoms becomes deeply quantum mechanical due to matter-wave interference and integrability [5, 12, 13].

This work studies fidelity decay of matterwaves in an ADKR potential under a momentum displacement [6]. The displacement operation is experimentally generated by a grating diffraction due to the atomic recoil effect in an atom interferometer [14, 15, 16]. We observe loss and revival of matter-wave coherence under a few ADKR kicks which saturates to a constant value insensitive to hundreds of kicks at quantum resonance. Our observation for the first time demonstrates stability of matterwaves in a classically-chaotic ADKR potential with a saturation of fidelity decay [5]. By introducing a “displacement diagram” to organize the total mutual coherence for wavepacket pairs in the interferometer, we provide an external-state extension of the formula developed in ref. [5, 11] and show excellent agreements between our observation and the theory. We also show that the saturation of fidelity is accompanied with an invariant distribution of matter-wave coherence which suggests interferometric applications of ADKR.

Our interferometry scheme follows those developed in ref. [16]. An optical SW is pulsed to create a sinusoidal light shift potential, that diffracts atoms into multiple diffraction orders, with n^{th} diffraction order weighted by amplitude $i^n J_n(\Theta)$. Here Θ is the interferometer SW pulse area, and J_n the n^{th} order Bessel function. Successive applications of two pulses at $t = 0$ and $t = T$ leads to a revival of atomic density grating at around time $t = 2T$. The revived atomic density grating has a k-vector $\mathbf{Q} = \mathbf{k}^a - \mathbf{k}^b$, that is the same as the k-vector of the interferometer SW which is composed of traveling light fields $E^{a,b}$ with k-vectors $\mathbf{k}^{a,b}$ [red/gray arrows in Fig. 1(a)]. A “grating echo” technique [16, 17] that monitors the Bragg scattering of light from the E^a mode into the E^b mode can retrieve the Fourier component of the atomic density grating ρ_{-Q} .

The matter-wave diffraction paths in the interferometer are sketched with a $x - t$ recoil diagram [18] in Fig. 1(a), where straight lines guide the centers of the diffracted wavepackets. The atomic density fringes at around time $t = 2T$ are due to the interference between pairs of wavepackets along adjacent diffraction paths that form “triangle loops”. Obviously, the relative displacements between the two diffraction paths in all these triangles are the same, due to the quantized recoil momentum $\hbar Q$ from the interferometer SW field. For a convenient

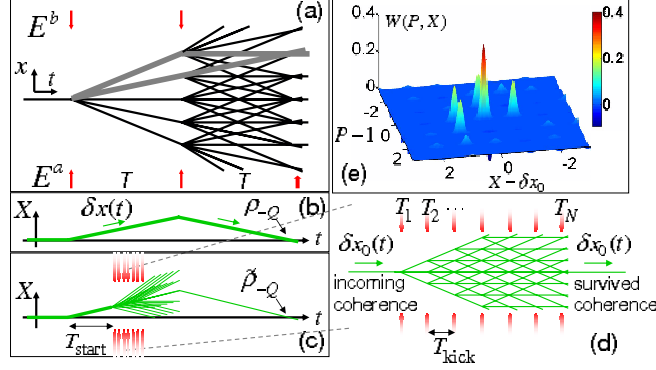


FIG. 1: (Color online) (a): Recoil diagram for a 3-pulse interferometer. (b): Diagram for the relative displacement between two interfering wavepackets of interest. (c): Displacement diagram of (b) perturbed by ADKR. (d): An expanded view of the interaction regime in (c) in a moving frame. Here $\delta x_0(t)$ corresponds to $\delta x(t)$ in (b) with $0 < t < T$. (e): 2D plot of a typical *invariant* distribution of $W(P, X)$ under ADKR around $P = \hbar(Q' = Q)$ and $X = \delta x_0(T_i)$ at quantum resonance (P and X is normalized to $\hbar Q$ and $\frac{\hbar Q}{m} T_{\text{kick}}$ respectively). The incoming coherence $W(P, X)$ is a Gaussian distribution with unity amplitude. The central peak corresponds to the survived coherence, given by Eq. (4) with $\phi = 1.6$.

discussion of the total mutual coherence between all these wavepacket pairs, we consider a “displacement diagram”, that only marks the relative displacement $\delta x(t)$ between these wavepacket pairs in a $X - t$ coordinate. The total mutual coherence between the wavepacket pairs induces a peak in the phase-space correlation function $W(P, X, t) = \text{Tr}[\hat{\rho}(t)\hat{D}(P, X)]$ at $P = \pm\hbar Q$ and $X = \delta x(t) = \int_0^t \frac{P}{m} dt$. Here $\hat{\rho}(t)$ is the single atom density matrix operator, $\hat{D}(P, X) = e^{i/\hbar(P\cdot\hat{x} - X\cdot\hat{p})}$ is a displacement operator (\hat{x} and \hat{p} is the position and momentum operator respectively) [19]. The $\delta x(t)$ in Fig. 1(b) will be referred to as “displacement lines” that guide peaks of the correlation function $W(P, X, t)$ in the displacement diagram. Using the properties of $\hat{D}(P, X)$, it is easy to show that the interaction of an impulse of SW $V(\hat{x}, t) = \hbar\theta \cos(Q'\hat{x})\delta(t)$ (with k-vector Q') leads to

$$W(P, X, 0^+) = \sum_n J_n \left(2\theta \sin \frac{Q'X}{2} \right) W(P - n\hbar Q', X, 0^-). \quad (1)$$

Thus the peaks of $W(P, X, t)$ can be shifted by multiples of $\hbar Q'$ along the P axis with a SW “diffraction”. Also, notice that an interference fringe is expected whenever the displacement line intersects the $X = 0$ axis, since the associated wavepacket pairs overlap in real space. In particular, we have the interferometer output $\rho_{-Q}(2T) = W(P = -\hbar Q, X = 0, t = 2T)$

[Fig. 1(b)].

We now consider the same interferometry sequence represented by Fig. 1(a), 1(b) to be perturbed by an ADKR potential, that is composed of N pulses of SW at a repetition rate of $1/T_{\text{kick}}$, starting at $t = T_{\text{start}}$ [red/gray arrows in Fig. 1(c), (d)]. We consider the kicked rotor SW with a grating k-vector Q' close but not exactly equal to Q , that is realized by introducing a small intersection angle between the kicked rotor SW and interferometer SW. The ADKR Hamiltonian is given by $H(\hat{p}, \hat{x}, t) = \hat{p}^2/2m + V_{\text{KR}}(\hat{x}, t)$ with

$$V_{\text{KR}}(\hat{x}, t) = \hbar\theta \cos(Q'\hat{x}) \sum_{i=1}^N \delta(t - T_i). \quad (2)$$

Here $T_i = T_{\text{start}} + (i-1)T_{\text{kick}}$ specifies $\{T_i\}$. The impact of ADKR generally leads to a reduction of interferometry fringe contrast from $\rho_{-Q}(2T)$ to $\tilde{\rho}_{-Q}(2T)$, due to the differential perturbation to the pairs of wavepackets. We define a dephasing factor $f = \tilde{\rho}_{-Q}(2T)/\rho_{-Q}(2T)$ to characterize the loss of the total mutual coherence. To express $f = f(\theta, \{T_i\})$ analytically we consider the displacement diagram in Fig. 1(c), with the interaction part expanded in Fig. 1(d) in a frame co-moving with $\delta x_0(t)$. Here $\delta x_0(t) = v_Q t$ corresponds to the unperturbed displacement line at $0 < t < T$ in Fig. 1(b). The matter-wave coherence contributing to the interferometry fringe is specified by $W(P, X)$ along $X = \delta x_0(t)$. Thus $f(\theta, \{T_i\})$ gives the fraction of the coherence that survives the ADKR perturbation in a network of displacement lines [Fig. 1(c), (d)], where peaks of $W(P, X)$ are scattered [due to Eq. (1)] and interfere at the vertex $(P^{(r)}, X^{(s)})$ in the moving frame. Here r, s are two integers, $P^{(r)} = r\hbar Q'$ and $X^{(s)} = s\frac{\hbar Q'}{m}T_{\text{kick}}$. By iteratively applying Eq. (1) at each vertex, we have the dephasing factor f ,

$$f(\theta, \{T_i\}) = \sum'_{\{n_i\}} \prod_{i=1}^N J_{n_i} \left(2\theta \sin \frac{Q'}{2} X_i^{\{n_i\}} \right). \quad (3)$$

Here $X_i^{\{n_i\}} - \delta x_0(T_i) \in \{X^{(s)}\}$, and n_i is the displacement diffraction order [Eq. (1)] at time T_i . A set of $\{n_i\}$ specifies a particular diffraction path in Fig. 1(d) while the sum in Eq. (3) is for all the paths satisfying $\sum n_i = r_N = 0$, $\sum (i-1)n_i = s_N = 0$.

We found it is particularly simple to analytically evaluate Eq. (3) at quantum resonance [12], with $T_{\text{kick}} = n\pi/\omega_{Q'}$ so that $X_i^{(n_i)} = \delta x_0(T_i) + 2sn\pi/Q'$, where n is an integer, $\omega_{Q'} = \hbar Q'^2/2m$ is the two-photon atomic recoil frequency and m is the atomic mass. By ignoring the negligible difference between $\omega_{Q'}$ and ω_Q , we found

$$f_{\text{QR}}(\phi, N) = \frac{1}{2\pi} \int_{-\pi}^{\pi} J_0 \left(\phi \frac{\sin(Ny/2)}{\sin(y/2)} \right) dy, \quad (4)$$

where $f_{\text{QR}}(\phi, N)$ gives $f = f(\theta, \{T_i\})$ when T_{kick} meets the quantum resonance and $\phi = 2\theta \sin(\omega_Q T_{\text{start}})$ is considered as the external-state counterpart of the differential perturbation strength for two internal states [5, 10, 11]. Equation (4) is remarkable: as suggested in ref. [5], in the large N limit $f_{\text{QR}} = \int_{-\pi/2}^{\pi/2} J_0[\phi \sec(\alpha)/2]^2 d\alpha/\pi > 0$. This means that a significant fraction of matter-wave coherence survives even after an infinite number of kicks, which requires a freeze or saturation of fidelity decay under the differential perturbation for majority of wavepackets in the interferometer [5, 6].

The experimental setup is similar to that in ref. [20]. Approximately 10^7 laser-cooled ^{87}Rb atoms in their ground state $F = 1$ hyperfine level are loaded into a magnetic guide oriented along \mathbf{e}_x , resulting in a cylindrically-shaped atom sample 1 cm-long and $170 \mu\text{m}$ -wide at $25 \mu\text{K}$ temperature. The interferometer SW, with k-vector precisely aligned along \mathbf{e}_x , is formed by two traveling waves E^a and E^b , detuned 120 MHz to the blue of the $F=1 - F'=2$ D2 transition. The interferometer SW is pulsed for 300 ns at $t = 0$ and $t = T$, with typical pulse areas of $\Theta \sim 1.5$. The total interrogation time $2T$ is chosen to be 6.066 ms or 12.165 ms in different experimental trials. The ADKR pulses are delivered by a different standing wave that is formed by retro-reflecting a traveling laser beam that is 6.8 GHz detuned to the red side of $F=1 - F'=2$ D2 transition, and is 40 mrad misaligned from the \mathbf{e}_x direction. This SW field is pulsed at $t = T_i$ according to Eq. (2), with 400 ns duration and has a typical pulse area $\theta \sim 0.1 - 1.3$. In ref. [20] we have shown that the magnetic confinement introduces negligible perturbation to the matter-wave interference along \mathbf{e}_x . Here we take advantage of the confinement to maintain the $170 \mu\text{m}$ transverse atomic sample distribution across the 2 mm-diameter ADKR laser beam, which enables a consistent ADKR interaction strength with up to $N = 150$ kicks. The ‘‘grating echo’’ signal amplitude is retrieved at around $t = 2T$ using a heterodyned technique [16, 17], recorded in repeated experiments as a certain parameter in ADKR is scanned. We normalize the grating echo amplitude with a reference signal level when no ADKR pulse is applied. The normalized amplitude $f = f(\theta, \{T_i\})$ corresponds to the dephasing factor in Eq. (3) in the ideal model. Due to the misalignment, the projection of ADKR k-vector along the interferometer SW direction \mathbf{e}_x gives $(\omega_Q - \omega_{Q'})/\omega_Q \sim 1.6 \times 10^{-3}$ that will be ignored in this paper. We normalize T_{start} , T_{kick} with respect to $2\pi / \langle \omega_{Q'} \rangle = 66.4 \mu\text{s}$ for a convenient comparison between theory and experiment.

The distinct behavior of interferometer contrast decay at different T_{kick} with increasing

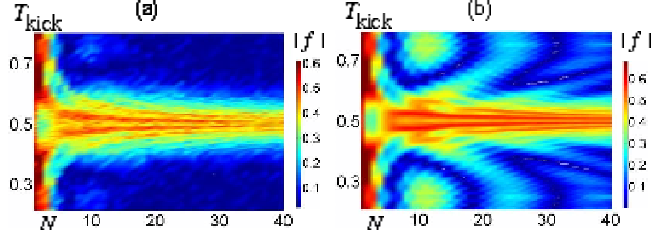


FIG. 2: (a): Experimentally observed dephasing factor $|f|$ with $N=1,\dots,40$. Here (normalized) $T_{\text{start}} = 0.25 + T_{\text{kick}}$. (b): Simulation of $|f|$ using Eq. (3) with $\theta = 0.7$.

N in ADKR is shown in Fig. 2(a). The kicked rotor SW pulse area was chosen to be $\theta = 0.7$, calibrated with independent measurements. The density plot in Fig. 2(a) composes 40×80 data points from repeated experiments, which scan T_{kick} from 0.21 to 0.8, and N from 1 to 40. From Fig. 2(a) we read the dephasing factor f according to the color coding, along the N axis at different T_{kick} . For T_{kick} far from 0.5, a rapid decay from $f = 1$ ($N=0$) down to zero (noise level) is observed. However, we see multiple “bright fringes” of high- f “flow” to the vicinity of $T_{\text{kick}} = 0.5$ with increasing N . At $T_{\text{kick}} = 0.5$, we see a quick loss of coherence from $f = 1$ to $f \sim 0.25$ at $N \sim 3$, which partly revives to $f \sim 0.45$ at $N \sim 5$, and then maintains the constant value without noticeable decay. In Fig. 2(b) we plot the results of simulation based on Eq. (3). We found a very good match between Fig. 2(a) and (b) both for small N , and for T_{kick} around 0.5 [22]. The discrepancy regimes in Fig. 2(a) and 2(b) is likely related to increased residual magnetic field perturbations due to atomic momentum diffusion [12], which is currently under experimental and theoretical investigations.

We accurately determine the kicked rotor SW recoil frequency ω_Q by minimizing the ADKR induced dephasing effect with T_{kick} at various T_{start} [21]. Here we fix $T_{\text{kick}} = 0.5$ to be at quantum resonance. According to Eq. (4), at quantum resonance a convenient parameter to characterize the differential perturbation is $\phi = 2\theta \sin \omega_Q T_{\text{start}}$. We fix θ and use T_{start} to control ϕ , and study the evolution of the dephasing factor f at an increasing number of kicks. The scatter plot in Fig. 3(a) gives four measurements of this type, up to $N = 60$. For comparison, we plot the theoretical expectation with solid lines, calculated according to Eq. (4). Here in the calculation $\theta = 1.22(5)$ is determined consistent with $\theta = 0.7$ in Fig. 2 according to a known kicked rotor SW intensity ratio calibrated with a photodiode. From Fig. 3(a) we see a loss, revival, and saturation of the dephasing factor f with increasing N at all perturbation strengths ϕ . The transient feature on the loss and revival of coherence

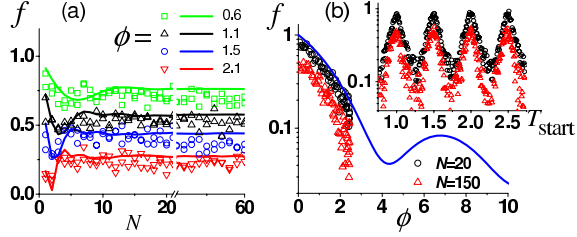


FIG. 3: (Color online) Dephasing factor f at $T_{\text{kick}} = 0.5$. Scatter plots give experimental data. Solid lines are calculated according to Eq. (4). (a): f vs N . (b): f vs ϕ . Inset gives the same experimental data plotted vs T_{start} .

happens more rapidly at larger ϕ . In case $\phi = 2.1$, the dephasing factor f approximately settles to the saturation value in only $N = 3$ kicks.

To study the dephasing factor f vs the differential perturbation strength ϕ in the saturation regime, we fix $\theta = 1.22$ and scan T_{start} at a fixed large number of kicks. Typical results are plotted in the inset of Fig. 3(b). We further plot f directly with ϕ in Fig. 3(b) with up to $\phi = 2.44$, limited by ADKR pulse strength in this experiment. Notice at $N = 150$, f only uniformly shifts downward by $\sim 40\%$ as compared with f at $N = 20$, indicating an independent coherence loss mechanism [21]. From Fig. 3(b) we see an excellent agreement between the observed dephasing factor in the saturation regime, and those calculated according to Eq. (4) at large N limit.

We come back to Fig. 1(d) and Eq. (3). Due to the kicked rotor pulses, matter-wave coherences specified by peaks of $W(P, X)$ are scattered and transported among 2D sites $(P^{(r)}, X^{(s)})$. The saturation of matter-wave coherence, as predicted by Eq. (4) and confirmed in Fig. 3, requires a distribution of $W(P, X)$ among these sites *invariant* under the ADKR actions. Figure 1(e) gives one example of the invariant distribution, calculated with an extension of Eq. (3) with general r_N, s_N at large N limit. The invariance of the 2D matter-wave coherence distribution under the ADKR action compliments the stable momentum population distribution when ADKR meets quantum resonance [12], and is clearly an interference effect in the ADKR scattering network [Fig. 1(d)]. By modifying the interferometry scheme to probe atomic fringes at $t = 2T \pm T_{\text{kick}}$, we have experimentally observed the coherence peaks displaced by $\pm v_Q T_{\text{kick}}$ along the X axis. The peaks displaced along the P axis by multiples of $\hbar Q$ can instead be probed by a “stimulated echo” [16]. The invariant distribution of coherence may be explored for robust manipulation of matter-waves in phase

space for interferometric applications.

In conclusion, we have observed a revival and saturation of matter-wave coherence with increasing number of ADKR kicks at or near the quantum resonance with an atom interferometer. Our experiments demonstrate that the wave interference rescues the classical instability of ADKR in the deep quantum regime where semi-classical pictures fail [5, 6], in excellent agreement with an external-state extension of fidelity decay theory discussed recently [5]. The ADKR in this work already corresponds to a classical Hamiltonian deep in the chaotic regime [2, 12]. Wave stability at or near quantum resonances in classically chaotic ADKR stems from the stability of the corresponding pseudo-classical map [10, 23]. By installing a chirped kicked rotor SW, we plan to explore stable structures in the pseudo-classical map due to Quantum Accelerator Modes [5, 10, 23], and search for invariant distribution of matter-wave coherence for precision measurements.

We thank E. J. Su for contributions to the interferometry setup, and C. Petitjean and E. J. Heller for very helpful discussions. This work is supported by MURI and DARPA from DOD, ONR and U.S. Department of the Army, Agreement Number W911NF-04-1-0032, by NSF, and by the Charles Stark Draper Laboratory.

* Current address: NIST, Gaithersburg, MD 20899

- [1] A. Peres, Phys. Rev. A **30**, 1610 (1984).
- [2] B. V. Chirikov, Phys. Rep. **52**, 263, (1979).
- [3] G. Veble *et al.*, Phys. Rev. Lett. **92**, 034101,(2004).
- [4] T. Gorin, T. Prozen *et al.*, Phys. Rep. **435**, 33 (2006).
- [5] S. Wimberger *et al.*, J. Phys. B **39**, L145 (2006).
- [6] C. Petitjean *et al.*, Phys. Rev. Lett. **98**, 164101 (2007).
- [7] H. M. Pastawski *et al.*, Phys. Rev. Lett. **75**, 4310 (1995).
- [8] N. Friedman *et al.*, Phys. Rev. Lett. **86**, 1518 (2001).
- [9] M. F. Andersen *et al.*, Phys. Rev. Lett. **97**, 1518 (2006).
- [10] S. Schlunk *et al.*, Phys. Rev. Lett. **90**, 054101 (2003).
- [11] F. Haug *et al.*, Phys. Rev. A **71**, 43803 (2005).
- [12] F. L. Moore *et al.*, Phys. Rev. Lett. **75**, 4598 (1995).

- [13] C. Ryu *et al.*, Phys. Rev. Lett. **96**, 160403 (2006).
- [14] *Atom interferometry*, edited by P. R. Berman (Academic Press, Cambridge, 1997).
- [15] D. W. Keith *et al.*, Phys. Rev. Lett. **66**, 2693 (1991).
- [16] S. B. Cahn *et al.*, Phys. Rev. Lett. **79**, 784 (1997). D. Strekalov *et al.*, Phys. Rev. A **66**, 23601 (2002).
- [17] T. W. Mossberg *et al.*, Phys. Rev. Lett. **43**, 851 (1979).
- [18] R. Friedberg *et al.*, Phys. Rev. A **48**, 851 (1993).
- [19] The widths of the induced peaks along P - and X - axis are given by the atomic coherence length in momentum and position space respectively. $W(P, X)$ is referred to as Weyl function. See S. Chountasis and A. Vourdas, Phys. Rev. A **58**, 848 (1998); S. Wu *et al.*, arXiv:0710.5479.
- [20] S. Wu, E. J. Su *et al.*, Phys. Rev. Lett. **99**, 173201 (2007). E. J. Su, S. Wu *et al.*, physics/0701018 (2007).
- [21] A. Tonyushkin, S. Wu, M. G. Prentiss, in preparation.
- [22] The observation is confirmed at $T_{\text{kick}} = n/2$ with $n > 1$.
- [23] S. Fishman *et al.*, Phys. Rev. Lett. **89**, 84101 (2002).